Phosphorylated Intrinsically Disordered Region of FACT Masks Its Nucleosomal DNA Binding Elements[*][S]

Yasuo Tsunaka[‡§], **Junko Toga**[‡], **Hiroto Yamaguchi**[‡], **Shin-ichi Tate**[¶], **Susumu Hirose**[∥], **and Kosuke Morikawa**[‡**1]

From the [‡]*Takara-Bio Endowed Laboratory, Institute for Protein Research, Osaka University, 6-2-3 Furuedai, Suita, Osaka 565-0874, Japan,* [§]*JSPS, Ichibancho, Chiyoda-ku, Tokyo 102-8472, Japan, the* [¶]*Department of Mathematical and Life Sciences, Graduate School of Science, Hiroshima University, 1-3-1 Kagamiyama, Higashi-Hiroshima 739-8526, Japan, the* [∥]*Department of Development Genetics, National Institute of Genetics, Mishima, Shizuoka-ken 411-8540, Japan, and* [**]*CREST, JST, Sanban-cho, Chiyoda-ku, Tokyo 102-0075, Japan*

FACT is a heterodimer of SPT16 and SSRP1, which each contain several conserved regions in the primary structure. The interaction of FACT with nucleosomes induces chromatin remodeling through the combinatorial action of its distinct functional protein regions. However, there is little mechanistic insight into how these regions cooperatively contribute to FACT functions, particularly regarding the recognition of nucleosomal DNA. Here, we report the identification of novel phosphorylation sites of *Drosophila melanogaster* FACT (dFACT) expressed in Sf9 cells. These sites are densely concentrated in the acidic intrinsically disordered (ID) region of the SSRP1 subunit and control nucleosomal DNA binding by dFACT. This region and the adjacent segment of the HMG domain form weak electrostatic intramolecular interactions, which is reinforced by the phosphorylation, thereby blocking DNA binding competitively. Importantly, this control mechanism appears to support rapid chromatin transactions during early embryogenesis through the dephosphorylation of some sites in the maternally transmitted dSSRP1.

FACT (facilitates chromatin transcription),[2] an evolutionarily conserved protein in eukaryotes, is a heterodimer consisting of structure-specific recognition protein-1 (SSRP1) and SPT16 with a larger molecular mass than SSRP1 (1, 2). FACT is classified as a chromatin-remodeling factor essential for various processes within nuclei, such as transcription, DNA replication, and DNA repair (1, 3–11). In the transcriptional process, FACT displaces histone H2A/H2B dimers from nucleosomes, thereby facilitating RNA polymerase II transcription (12). The FACT

subunits also display a range of physical and genetic interactions with other factors (2, 3, 6, 11, 13), suggesting that FACT directs several different functions by interacting with multiple complexes.

At the molecular level, FACT initially binds nucleosomes and/or nucleosomal DNA, and then destabilizes the interactions between the H2A/H2B dimers and the H3/H4 tetramer within nucleosomes (2). Therefore, most studies have so far focused on interactions between FACT and histones. For example, it has been previously reported that the C-terminal region of human SPT16 (hSPT16) directly binds to H2A/H2B dimers (12). A recent study has revealed that the N-terminal amino peptidase-like domain of *Schizosaccharomyces pombe* SPT16 associates with the H3/H4 histones, suggesting that this SPT16 may contribute to binding, eviction, and/or deposition of all histones (14). However, it remains unclear how the FACT protein interacts with the nucleosomal DNA at the initial step of chromatin remodeling, although several studies have reported that the high-mobility group (HMG) box domain of SSRP1 binds to DNA nonspecifically or by recognizing specific structures of DNA (15–17).

The heterodimeric FACT complex consists of several distinct structural domains and intrinsically disordered (ID) regions (Fig. 1*A*). The functional aspects of these folded domains or unstructured regions have not been clarified yet. The smaller subunit, SSRP1, is categorized as a member of the HMG family (16), and is essential for cell (18) and animal (19) viability. This protein contains two structural domains, a structure-specific recognition (SSRC) motif (amino acids 186–436 in *Drosophila*) and an HMG-box domain (amino acids 555–624 in *Drosophila*). In yeast, the bipartite SSRP1 analog consists of Pob3 and Nhp6 (20). Further sequence analysis revealed that the other regions could be distinguished as four evolutionarily conserved regions: an N-terminal region (amino acids 1–186 in *Drosophila*), an acidic ID region (amino acids 437–518 in *Drosophila*) with limited homology to nucleolin, an HMG-flanking basic ID segment (amino acids 519–554 in *Drosophila*), and a mixed charge ID region at the extreme C terminus (amino acids 625–723 in *Drosophila*). SSRP1 initially acts on the nucleosomal DNA in the chromatin remodeling process through the combinatorial action of its distinct functional protein regions, such as the HMG domain. It is thus crucial to clarify the molecular mechanism by which SSRP1 interacts with the nucleosomal DNA. Furthermore, while several studies have reported the
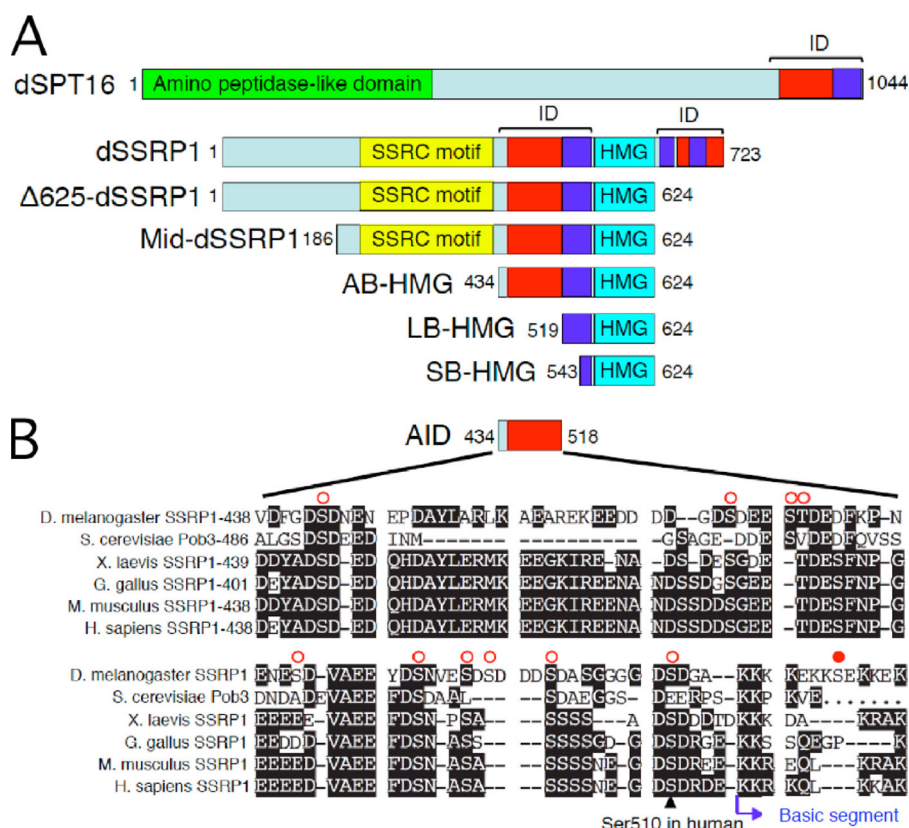
FIGURE 1. **dFACT domain organization and sequence alignment.** *A*, schematic representation of dSSRP1 deletion mutants. The acidic and basic amino acid enriched regions of dFACT are highlighted in *red* and *blue*, respectively. ID indicates the intrinsically disordered regions predicted by sequence analysis using the GTOP data base (54). *B*, alignment of acidic ID regions of SSRP1s. *Red open circles* represent the phosphorylation sites of dSSRP1 expressed in Sf9 cells, while the *red filled circle* is not phosphorylated. Ser-510 of hSSRP1 is the CK2 phosphorylation site *in vitro*, which affects the DNA binding function. This acidic region contains 36 acidic and 6 basic residues, and the following basic segment has 7 acidic and 22 basic residues in *Drosophila*.

nificance of these findings is highlighted by our observation that some phosphorylation sites in the maternally transmitted dSSRP1 were dephosphorylated immediately after fertilization to accommodate rapid chromatin transactions during early embryogenesis.

EXPERIMENTAL PROCEDURES

Plasmid Construction—We used the same dFACT cDNA as in our previous study (11). To obtain the His-tagged DNA sequences, the cDNAs encoding dSPT16 and dSSRP1 were cloned into the NdeI and XhoI sites of pColdI (Takarabio). To construct the plasmid for dSSRP1 and dSPT16 co-expression, the His-tagged dSPT16 DNA was ligated into the EcoRI and SalI sites downstream of the PH promoter in the pFastBacDual plasmid (Invitrogen), and then the dSSRP1 DNA was cloned into the XhoI and SphI sites under the control of the p10 promoter in the same plasmid. His-tagged deletion constructs of dSSRP1 were generated in pColdI (Δ625-dSSRP1 and Mid-dSSRP1; Fig. 1*A*) or pET28a (AB-HMG, LB-HMG, SB-HMG, and AID, Fig. 1*A*). The His-tagged Mid-dSSRP1 con-

phosphorylation of SSRP1 (8, 21–23), it remains unclear how the phosphorylation of SSRP1 affects DNA binding.

The ID regions of FACT are particularly intriguing. For instance, the C termini of SSRP1 and SPT16 consist of separate segments abundant in positive and negative charges (Fig. 1*A*). In fact, it has been demonstrated that the ID region of SPT16 is essential for the mRNA transcriptional elongation dictated by FACT (12). These disordered regions lack well-defined three-dimensional structures, but in some proteins they fold into ordered conformations upon binding to their extrinsic targets (24–26). Recently, we have successfully visualized the ID regions of *Drosophila melanogaster* FACT (dFACT) in solution by high speed atomic force microscopy (AFM) (27). However, the dynamic and functional behaviors of the FACT ID regions remain unknown at the molecular level.

Using the dFACT proteins expressed in Sf9 cells, we investigated how the phosphorylation of dSSRP1 (*D. melanogaster* SSRP1) induces the inhibition of DNA binding. Mutational analyses demonstrated that the phosphorylation sites regulating the nucleosomal DNA binding activity are concentrated in the acidic ID region of dSSRP1. This acidic ID region forms an intramolecular interaction with both the HMG domain and the basic ID segment. Notably, phosphorylation of the acidic ID region markedly strengthens this interaction, thereby blocking the DNA binding to the HMG domain. The physiological sig-

struct was also cloned into the XhoI and SphI sites under the control of the p10 promoter in pFastBacDual. To obtain the Ser/Thr to Ala mutants and the Δ624-dSSRP1 deletion, site-directed mutagenesis of the dFACT proteins was performed using the QuikChange site-directed mutagenesis method (Stratagene). To produce the Sf9-AB-HMG and Sf9-AID proteins, the protease site insertions within the Mid-dSSRP1 protein (thrombin and factor Xa sites inserted between amino acid residues 433–434 and 518–519, respectively) were also performed, using the same mutagenesis method.

Expression and Purification—Competent *Escherichia coli* DH10BAC cells (Invitrogen), transformed by these plasmids, were used to generate recombinant bacmids. The bacmid-cellfection complex was transfected into Sf9 cells. The Sf9 insect cells (ovary-derived cells from *Spodoptera frugiperda*) were propagated and maintained at 27 °C in Sf-900 II serum-free medium (Invitrogen). The baculovirus was collected at 72-h postinfection. The dFACT proteins were expressed at 27 °C for 48 h in Sf9 cells, which were infected at a density of 2×10^6 cells/cm^2 with the baculovirus including the dFACT cDNAs. The infected cells were collected by centrifugation and were suspended in lysis buffer containing 0.15 M NaCl, 20 mM Tris-HCl, pH 8.5, 0.1% Nonidet P-40, and a protease inhibitor mixture (Nacalai-Tesque). After clarification of the lysate by two rounds of centrifugation at 15,000 rpm for 30 min, the super-

Inhibition by FACT ID Phosphorylation

natant was loaded onto a Histrap column (GE Healthcare). After washing the column with buffer A (20 mM Tris-HCl, pH 8.5, 5 mM 2-mercaptoethanol) containing 20 mM imidazole and 0.6 M NaCl, the bound proteins were eluted with buffer A containing 0.5 M imidazole and 0.15 M NaCl. The proteins were then applied to a Hitrap Q exchange column (GE Healthcare), which was eluted with a concentration gradient of 0.15–1 M sodium chloride in buffer A. Peak fractions containing the FACT complex were dialyzed against buffer A containing 0.15 M NaCl, and then were purified on a Hitrap Heparin column (GE Healthcare) by elution with a concentration gradient of 0.15–1 M sodium chloride in buffer A. The expression and purification of dFACT proteins from *E. coli* have been described previously (27, 28).

The purification of the Sf9-AID and Sf9-AB-HMG proteins was impossible due to their very low expression levels in the baculovirus insect cells. Thus, we expressed the Sf9-Mid-dSSRP1 protein with two protease sites (a thrombin site between amino acid residues 433 and 434, and a factor Xa site between amino acid residues 518 and 519) in Sf9 cells, and then treated them with thrombin and factor Xa to generate these desired proteins. First, the purified Sf9-Mid-dSSRP1 protein with two protease sites was cleaved with thrombin for 16 h at 4 °C. The resultant protein mixture was applied to a Histrap column equilibrated in buffer A containing 0.15 M NaCl, and the flow-through fraction contained the desired Sf9-AB-HMG protein. The Sf9-AB-HMG protein was further purified on a Hitrap Q exchange column by elution with a concentration gradient of 0.15–1 M sodium chloride in buffer A. Next, this Sf9-AB-HMG protein was cleaved with factor Xa for 16 h at 4 °C during dialysis against buffer A containing 0.15 M NaCl. The resultant protein mixture was applied to a Hitrap Q exchange column equilibrated in buffer A containing 0.15 M NaCl. The desired Sf9-AID protein was eluted with a concentration gradient of 0.15–1 M sodium chloride in buffer A. All of the purified proteins were dialyzed against buffer A containing 0.15 M NaCl.

Protein Extraction from Ovaries and Embryos—We used the same fly stocks as in the previous study (11). Embryos 0–1, 1–3, and 0–3 h after egg laying (AEL) were collected from a population reared at 25 °C, and were dechorionated. Ovaries were extirpated from the abdominal segment of adult female flies from the same population in cold buffer, containing 130 mM NaCl, 5 mM KCl, 2 mM CaCl$_2$, and 10 mM HEPES, pH 6.0. The ovaries and embryos were homogenized in cytosolic extract buffer, containing 50 mM NaCl, 20 mM Tris-HCl, pH 7.9, 3 mM MgCl$_2$, 0.5 mM dithiothreitol, 0.5 mM phenylmethylsulfonyl fluoride, 5% glycerol, 0.3% Nonidet P-40, and a protease inhibitor mixture (Sigma), and after centrifugation, the supernatant was saved as the cytosolic extract. The nuclear pellet was then treated with nuclear extract buffer (the same composition as cytosolic extract buffer, except for 0.5 M NaCl) to yield the nuclear extract.

APase Reaction—dFACT proteins (300 pmol) were incubated with 15 units of calf intestine alkaline phosphatase (Takara-bio), in reaction mixtures containing 50 mM Tris-HCl, pH 9.0, and 1 mM MgCl$_2$, at 20 °C for 2 h.

Analysis of Phosphorylation States by Native-PAGE—The purified dFACT heterodimers and the extracts from ovaries and embryos were denatured with urea buffer (8 M urea, 20 mM Tris-HCl, pH 8.5, 100 mM NaCl). These samples were fractioned by 5% native-PAGE in Tris-glycine buffer, and then were detected on Western blot with anti-dSSRP1 antibodies. We used the same anti-dSSRP1 antibodies as in the previous study (11).

Analysis of Phosphorylation States by Two-dimensional Gel Electrophoresis—Proteins (20 μg) were loaded onto 4–7 IPG strips (GE Healthcare) in rehydration solution (8 M urea, 2% CHAPS, 20 mM dithiothreitol, 0.5% 4–7 IPG buffer (GE Healthcare)). Iso-electric focusing was performed using IPG strips in Ettan IPGphor II system (GE Healthcare). After first dimension run was completed, IPG strips were transferred onto gels and subjected to 10% SDS-PAGE. The samples were detected by CBB stain.

Electrophoresis Mobility Shift Assays (EMSAs)—Recombinant human full-length histone proteins were produced in *E. coli* and purified as reported previously (29). Mononucleosomes were reconstituted from histones and a 146 bp or a 263 bp DNA with the strongest positioning sequences (30, 31). The 263-bp DNA fragment containing the nucleosome positioning sequence 601 was prepared by PCR from pGEM3Z-601 (kindly provided by J. Widom) (31). The 146-bp palindromic DNA fragment (30), derived from a human α-satellite region, was constructed and purified as described previously (32). Mononucleosomes were assembled by a salt dialysis method using these core histones and the 146-bp or 263-bp DNA fragments and were purified by chromatography on a Mini Q column, as described previously (29).

Purified mononucleosomes were incubated with the FACT proteins, in reaction mixtures containing 20 mM Tris-HCl, pH 8.0, 0.1 mM EDTA, 150 mM NaCl, and 5 mM 2-mercaptoethanol at 20 °C for 5 min. The samples containing the full-length dSSRP1 were electrophoresed at 4 °C on a 0.7% agarose gel in 0.5× TBE, and then were visualized by SYBR Gold nucleic acid gel stain. Each band was quantified using the ImageJ v1.41o (United States National Institutes of Health). The Mid-dSSRP1 was fractionated by 5% PAGE in 0.2× TBE.

Competitive Binding Assay on Native-PAGE—A 20-base pair (bp) dsDNA fragment (5'-GCATAAATACGCATAAATAC-3') (0.1 nmol) was incubated with an equimolar amount of the proteins for 5 min at 20 °C, in reaction mixtures containing 20 mM Tris-HCl, pH 8.0, 0.1 mM EDTA, 150 mM NaCl, and 5 mM 2-mercaptoethanol. AID proteins (0.1 nmol) were also incubated with an equimolar amount of LB-HMG for 10 min at 20 °C in the same reaction mixtures. In the competitive assay, AID proteins (0.1 nmol) were preincubated with an equimolar amount of LB-HMG for 10 min at 20 °C. The resultant complexes were titrated with 0.3, 1.0, 3.0, and 10.0-fold amounts of dsDNA, and then were incubated for 5 min at 20 °C under the same buffer conditions. The samples were fractionated at 4 °C by 15% native-PAGE in Tris-glycine buffer, and then were detected by CBB stain, EtBr stain, and ProQ-Diamond phosphoprotein stain.

NMR Spectroscopy—*E. coli* BL21 (DE3) cells, transformed by the SB-HMG protein expression plasmid, were cultured in M9
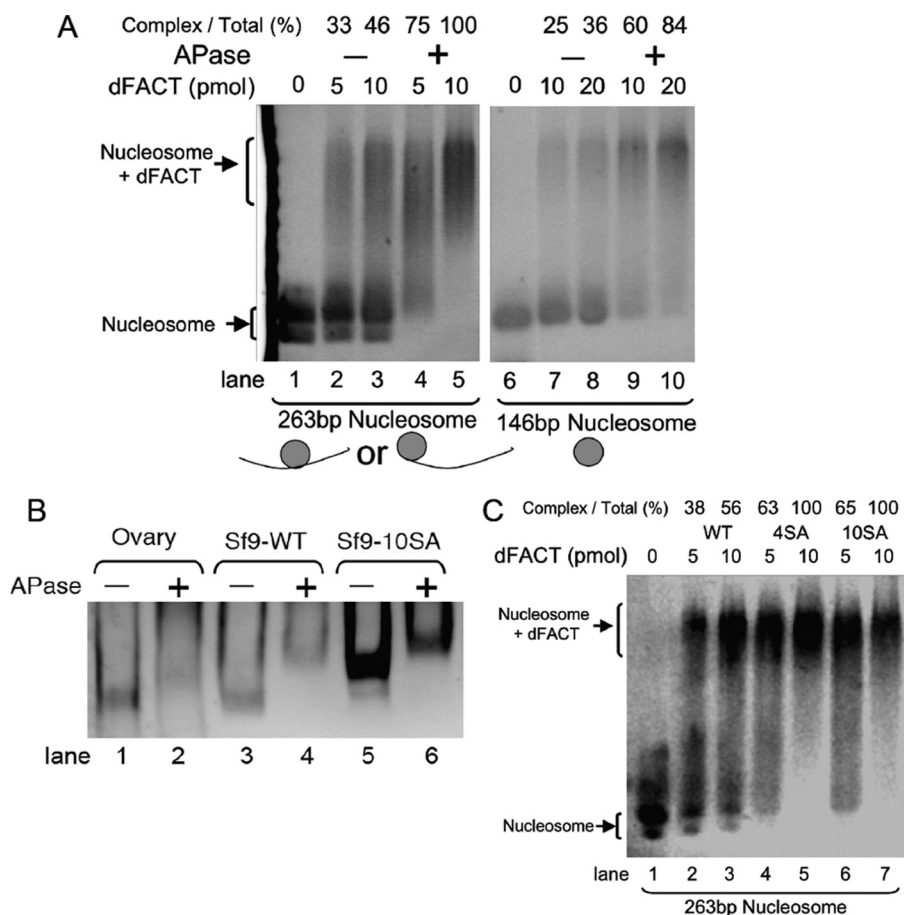
FIGURE 2. **Phosphorylated dFACT cannot bind to mononucleosomes.** *A*, EMSA for binding of WT-dFACT to 146 bp and 263 bp mononucleosomes. The proteins were preincubated with buffer (−) or APase (+) for 2h at 20 °C. An aliquot of 146 bp mononucleosomes (0.2 pmol) was incubated in 10 μl of reaction mixture with buffer (0), 10 pmol, or 20 pmol of the proteins for 5 min at 20 °C. For the 0.2-pmol aliquot of 263-bp nucleosomes, 5 and 10 pmol of protein were used. The samples were then analyzed by 0.7% agarose gel electrophoresis and were detected by SYBR Gold nucleic acid gel stain. Quantification of each band was carried out using the ImageJ. The percent of the complex band in the total (the complex and free nucleosome) is shown by the "Complex/Total" value (%) of each lane. As reported previously (48), the 263-bp nucleosomes show two bands, which correspond to the distinct positions of the histone octamer at one end and the middle of the DNA, respectively. *B*, analysis for the phosphorylation level of dSSRP1 proteins by 5% native-PAGE. Sf9-WT and Sf9−10SA are the wild-type and the S443A/S472A/S476A/T477A/S488A/S496A/S500A/S502A/S506A/S515A dFACT proteins, purified from Sf9 cells, respectively. *Ovary* represents a cytosolic fraction, extracted from fly ovaries. The dFACT complexes were dissociated with a buffer containing 8 M urea. The samples were analyzed by Western blotting with anti-dSSRP1 antibodies. *C*, EMSA for the effects of phosphorylation on binding between 263-bp mononucleosomes and dFACTs. *4SA* indicates the S500A/S502A/S506A/S515A mutants of dFACT.

minimal medium containing $^{15}NH_4Cl$ as the sole nitrogen source to produce the uniformly ^{15}N-labeled protein. The purified protein was dissolved in a solution, containing 5 mM Tris-HCl, pH 7.5, 50 mM KCl, and 10 mM $MgCl_2$ in 95% H_2O, 5% D_2O. The AID protein was also dissolved in the same buffer solution, containing 5 mM Tris-HCl, pH 7.5, 50 mM KCl, and 10 mM $MgCl_2$. The backbone ^1H, ^{15}N, $^{13}C\alpha$, $^{13}C\beta$, $^{13}C'$ resonances for the SB-HMG protein in the above solution were assigned using HNCO, HNCA, HN(CO)A, HNCACB, and CBCA-(CO)NH triple resonance experiments performed with a 600MHz spectrometer, Bruker DMX600 (33). A series of ^1H-^{15}N HSQC spectra were collected for samples with different molar ratios of SB-HMG to the AID protein. The molar ratios of the AID protein to SB-HMG were set to 0.1, 0.2, 0.5, 1.0, 1.5, and 2.0 *versus* the 0.1 mM SB-HMG concentration. The spectra were collected on a DMX750 spectrometer operating at 750

MHz for the ^1H resonance frequency, at 25 °C. All NMR data were processed with the program NMRPipe (34). Peak positions were elucidated by using contour simulation in the program PIPP (35), which calculated the peak position as an average of centers of simulated contour circles for all displayed contour levels. The chemical shift differences were calculated in Hz units in Equation 1,

$$\Delta\delta = \{[(\delta^1H_{bound} - \delta^1H_{free}) \times Fr(^1H)]^2 + [(\delta^{15}N_{bound} - \delta^{15}N_{free}) \times Fr(^{15}N)]^2\}^{1/2} \quad \text{(Eq. 1)}$$

where δ^1H_{bound} and δ^1H_{free} are the ^1H chemical shifts in ppm for the bound and ligand-free states, respectively. $\delta^{15}N_{bound}$ and $\delta^{15}N_{free}$ denote the counterparts for the ^{15}N chemical shifts. $Fr(^1H)$ and $Fr(^{15}N)$ were set to 749.93 and 75.99 in the present experiments performed on a 750 MHz spectrometer.

RESULTS

The Phosphorylated Form of FACT in Sf9 Cells Inhibits the Nucleosomal DNA Binding Activity—When dSSRP1 and dSPT16 (*D. melanogaster* SPT16) were co-expressed in the baculovirus-Sf9 insect cell system and purified from a cytosolic fraction of Sf9 cells, we obtained the full-length dFACT as a 1:1 complex between dSSRP1 and dSPT16 (Sf9-dFACT, supplemental Fig. S1). The Sf9-dFACT bound only 36–46% to 146 bp and 263 bp mononucleosomes, even at 1 μM.

(Fig. 2*A*, *lanes 3* and *8*). This could be due to phosphorylation of dFACT, as phosphorylation of hSSRP1 by casein kinase 2 (CK2) inhibited the nonspecific DNA binding activity of FACT (8). To examine this possibility, the Sf9-dFACT protein was treated with calf intestine alkaline phosphatase (APase), and then the dSSRP1, dissociated from the dFACT complex with 8 M urea, was subjected to native-PAGE. The APase treatment caused the gel mobility of dSSRP1 to become slower, suggesting that APase had removed some of the negatively charged phosphate groups of dSSRP1 (Fig. 2*B*, *lane 3 versus lane 4*). The dFACT, dephosphorylated with APase, recovered the nucleosomal DNA-binding activity, as compared with the phosphorylated form (Fig. 2*A*, *lanes 2* and *3 versus lanes 4* and *5*; *lanes 7* and *8 versus lanes 9* and *10*). Therefore, we concluded that the phosphorylation of dFACT inhibits its binding to nucleosomal DNA.
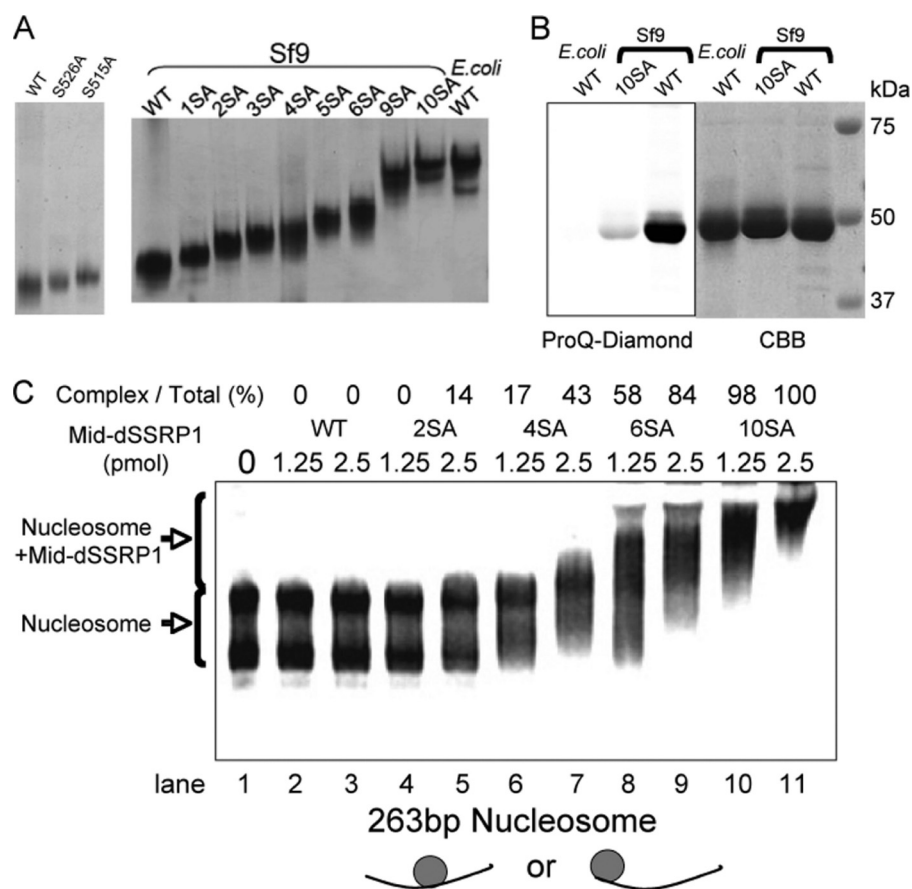
Inhibition by FACT ID Phosphorylation

FIGURE 3. **Identification of phosphorylation sites using Mid-dSSRP1 mutants.** *A*, analysis for the phosphorylation level of the potential phosphorylation site mutants of Mid-dSSRP1 proteins in 5% native-PAGE. *1SA, 2SA, 3SA, 4SA, 5SA, 6SA, 9SA, 10SA* represent the S515A, 1SA+S506A, 2SA+S502A, 3SA+S500A, 4SA+S496A, 5SA+S488A, 6SA+S472A/S476A/T477A, 9SA+S443A mutants of Mid-dSSRP1, respectively. Sf9 and *E. coli* labels are for the dFACT proteins expressed in Sf9 cells and *E. coli*, respectively. *B*, CBB (*right*) and ProQ-Diamond (*left*) staining of purified Mid-dSSRP1 proteins after 10% SDS-PAGE. The molecular mass is depicted in kDa. *C*, EMSA for binding of Mid-dSSRP1 proteins to 263-bp mononucleosomes by 5% PAGE. The incubation was performed as in Fig. 2A, except that 1.25 and 2.5 pmol of the proteins were used for 263-bp nucleosomes (0.2pmol). Quantification of each band was carried out using the ImageJ. The percent of the complex band in the total (the complex and free nucleosome) is shown by the *Complex/Total* value (%) of each lane. The 263-bp nucleosomes show two bands, which correspond to the distinct positions of the histone octamer at one end and the middle of the DNA, respectively.

Identification of Phosphorylation Sites Regulating the Nucleosomal DNA Binding Activity—The previous study has suggested that among the three residues identified as CK2 phosphorylation sites *in vitro*, the phosphorylation of serine 510 alone plays a crucial role in binding between hSSRP1 and DNA (8). This led us to search for the functional phosphorylation sites in dSSRP1 responsible for inhibiting the nucleosomal DNA binding. An extensive sequence alignment around Ser-510 of hSSRP1 revealed 11 potential phosphorylation sites (Fig. 1B; *red open* and *filled circles*) of dSSRP1 as CK2 target sequences ((S/T)XX(D/E) or (S/T)(D/E)). To find the actual phosphorylation sites in living cells, mutational analyses were carried out using native-PAGE and Ser/Thr to Ala mutants in Mid-dSSRP1 (Fig. 1A), which consists of the SSRC motif, the acidic region, the following basic segment, and the HMG domain. These analyses would reveal phosphorylation sites, because mutations from Ser/Thr to Ala of actual sites result in slower band migration than that for the wild-type (Fig. 3A). For example, the Ala mutation of the actual phosphorylation site (S515A) resulted in slower migration of the band than those of the WT and the S526A mutant (Fig. 3A, *left*). Except for Ser-526 (Fig. 1B, *red filled circle*) in the basic segment, ten sites (Fig. 1B, *red open circles*) were found to be phosphorylated in Sf9 cells. The mutant protein, whose actual phosphorylation sites were entirely replaced by Ala (10SA-Mid-dSSRP1), exhibited almost the same gel mobility as the unmodified wild-type protein expressed in *E. coli* (Eco-WT-Mid-dSSRP1) (Fig. 3A, *right*). Various mutants, in which the ten actual sites were replaced to different degrees (1SA, 2SA, 3SA, 4SA, 5SA, 6SA, and 9SA-Mid-dSSRP1), exhibited band shifts, as they stepwise got closer to that of Eco-WT-Mid-dSSRP1 (Fig. 3A, *right*).

To determine the phosphorylation sites more rigorously, we performed similar analyses using two-dimensional gel electrophoresis and Mid-dSSRP1 (supplemental Fig. S3). The spots of S506A and S506A/S515A mutants (R_f value of 0.39 and 0.41, respectively) stepwise got closer to the cathode side than that of WT (R_f value of 0.38), according to the number of mutation sites (supplemental Fig. S3, *spots 1 versus 2 versus 3*). The 10SA mutant (R_f value of 0.54) exhibited the spot migration closest to the cathode side (supplemental Fig. S3, *spot 4*). The 10SA mutant also exhibited subtle staining by using a ProQ-diamond

Next, we analyzed the competitive binding of the dephosphorylated dFACT between the nucleosome and dsDNA (supplemental Fig. S2). The nucleosome complex with dFACT was dissociated upon the addition of dsDNA, as revealed by the appearance of free nucleosomes (supplemental Fig. S2, *lanes 3–5*). These results demonstrate that the increased interaction is due to an increase in nonspecific DNA binding. In addition, the dephosphorylated dFACT more strongly interacts with nucleosomes that contain linker DNA, in agreement with the finding that HMG-box proteins bind to linker DNA. For example, the interaction with the 146-bp nucleosome, which completely lacks linker DNAs, required higher dFACT concentrations than that with the 263-bp nucleosome carrying linker DNAs (Fig. 2A, *lanes 4* and *5 versus lane 9* and *10*). However, this result is not consistent with the previous data that the linker DNA did not promote the binding of the yeast SPT16-Pob3-Nhp6A complex (36). This discrepancy may be due to the fact that metazoan FACTs contain the HMG domain within the single polypeptide of dSSRP1, while the domain is on a separate polypeptide in the yeast FACT complex.
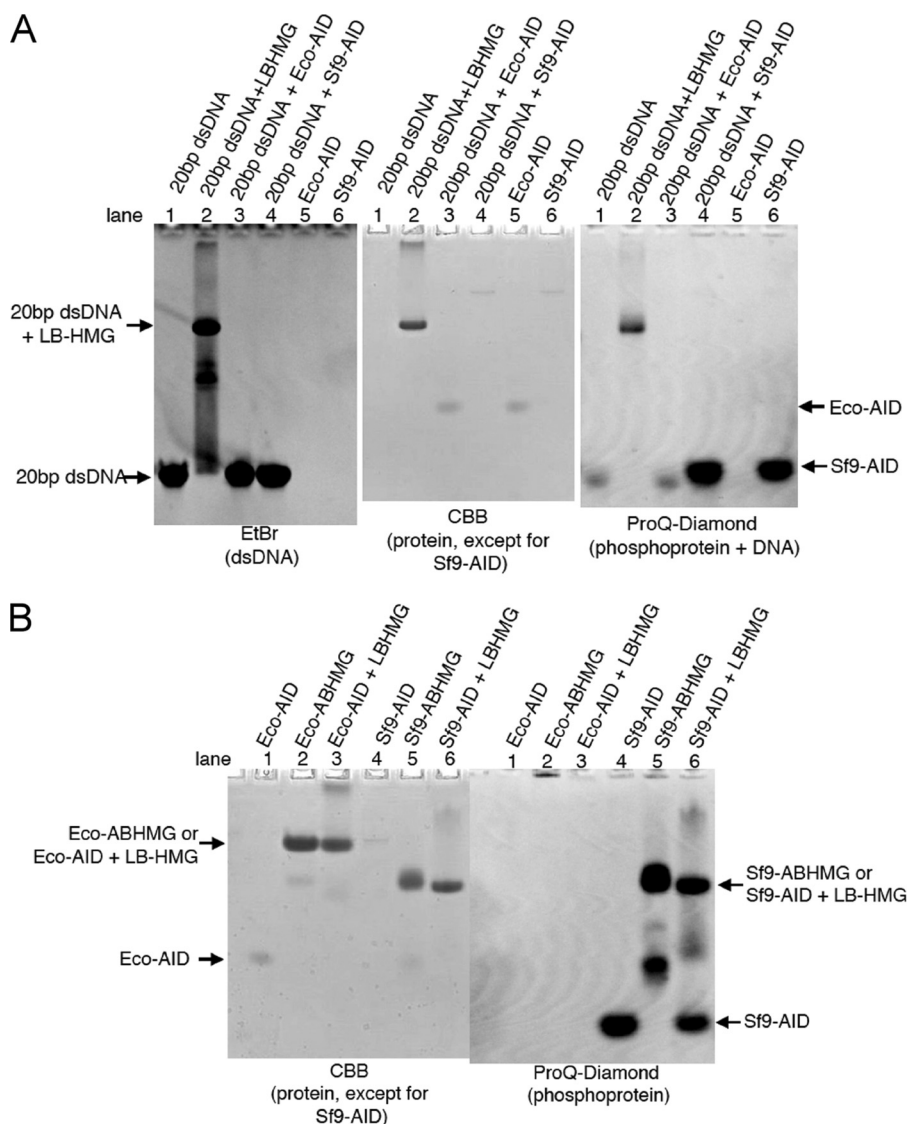
FIGURE 4. **The acidic ID region interacts with intramolecular HMG domain, but not with DNA.** *A*, EtBr (*left*), CBB (*center*), and ProQ-Diamond (*right*) staining of dSSRP1 deletion mutants and DNA complexes after 15% native-PAGE. *Sf9-* and *Eco-* labels refer to the proteins expressed in Sf9 cells and *E. coli*, respectively. A 20-bp dsDNA fragment (0.1 nmol) was incubated with equimolar amounts of the proteins for 5 min at 20 °C. Because CBB associates with protonated amino groups, the Eco-AID protein, including the highly negative charge cluster, showed weaker staining. The Sf9-AID protein consists of highly phosphorylated sites and negatively charged residues, and hence could not be stained by CBB. Therefore, the phosphoprotein bands were detected by the Pro-Q Diamond kit. *B*, CBB (*left*), and ProQ-Diamond (*right*) staining of dSSRP1 deletion mutants and the complexes after 15% native-PAGE. AID proteins (0.1 nmol) were incubated with an equimolar amount of LB-HMG for 10 min at 20 °C.
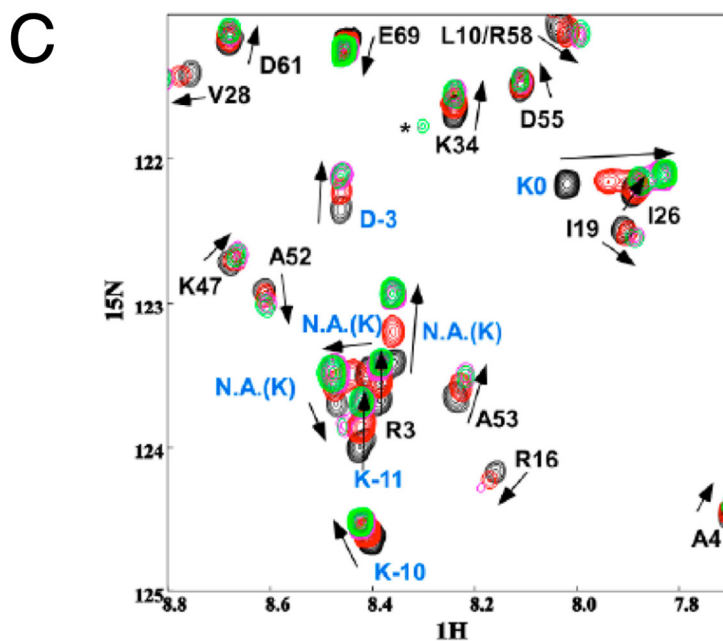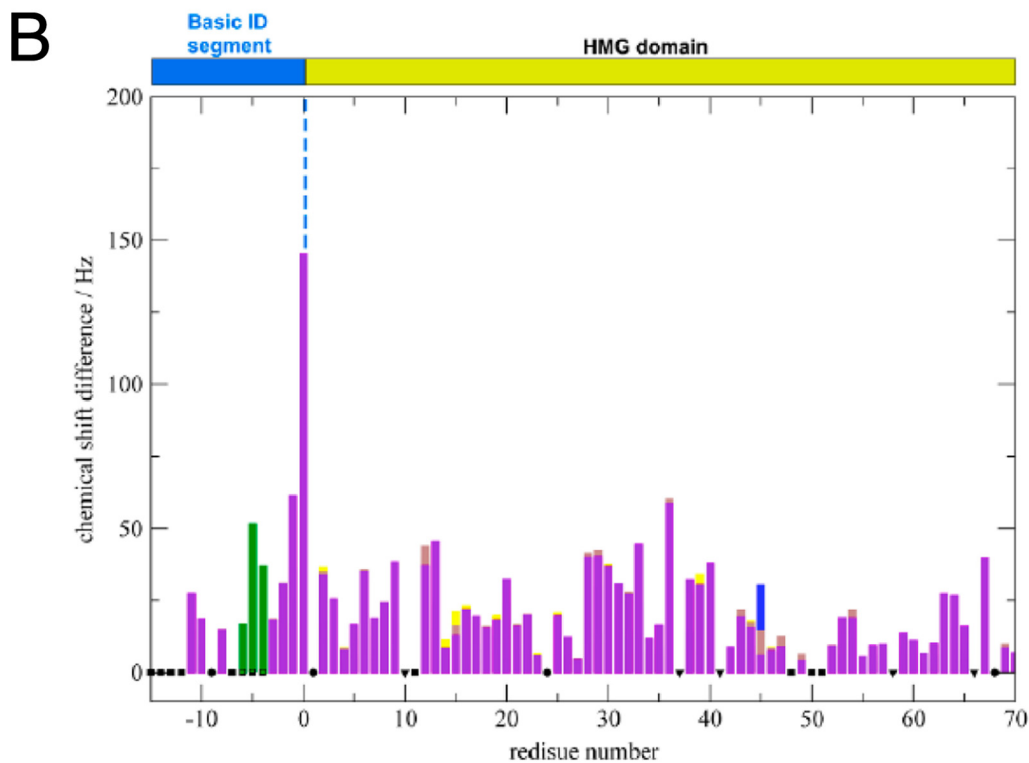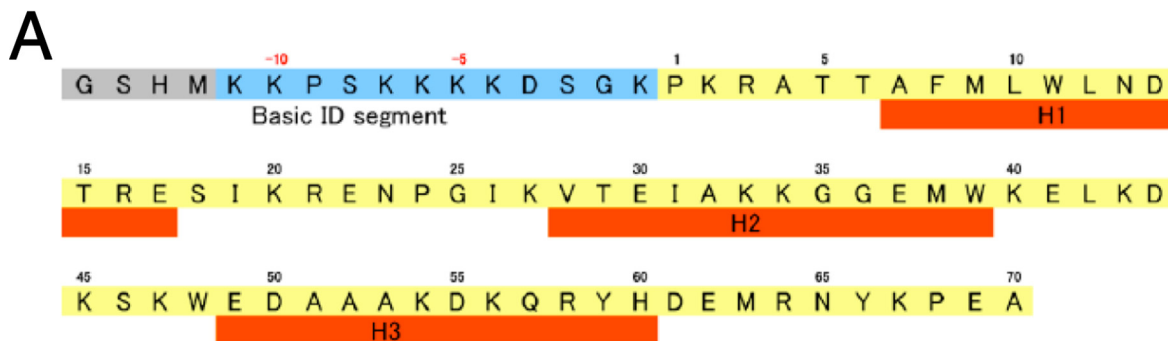
dSSRP1) were reduced, according to the decrease in the number of mutations at the phosphorylation sites (Fig. 3*C*, *lanes 4–11*).

Using the full-length dFACT complex, we also examined whether these sites are phosphorylated to regulate the nucleosomal DNA binding activity. In agreement with the results obtained with the dephosphorylated WT-dSSRP1, the 10SA-dSSRP1 protein, dissociated from the dFACT complex in the presence of 8 M urea, migrated more slowly on the native-PAGE than the fully phosphorylated WT protein (Fig. 2*B*, *lane 5 versus lane 3*). We also found that the full-length 4SA and 10SA-dFACT proteins bound to 263-bp nucleosomes with higher affinity than the WT protein (Fig. 2*C*, *lanes 4–7 versus lanes 2* and *3*). Although we found that the C-terminal region of dSSRP1 (amino acids 625–723) still contains other phosphorylation sites (Fig. 2*B*, *lane 5 versus lane 6* and supplemental Fig. S4*A*), its phosphorylation plays no major role in the inhibition of nucleosomal DNA binding (supplemental Fig. S4*B*). For example, the dFACT mutant complex, consisting of WT-Δ625-dSSRP1, exhibited low affinity to the nucleosomes, in comparison with the full-length WT-dFACT (supplemental Fig. S4*B*, *lanes 2* and *3 versus* Fig. 2*C*, *lanes 2* and *3*). Furthermore, the 10SA-Δ625 mutant recovered the nucleosomal DNA binding activity, despite the deletion of the C-terminal region (supplemental Fig. S4*B*, *lanes 4* and *5 versus lanes 2* and *3*). Therefore, it is likely that the C-terminal region of dSSRP1 has a positive effect on the interaction between dFACT and nucleosomes, but not an inhibitory one. These results suggested that the affinity of dFACT for nucleosomal DNA is regulated by phosphorylation or dephosphorylation at the ten sites within the acidic ID region.

The Acidic ID Region with the Clustered Phosphorylation Sites Interacts with the Intramolecular HMG Domain and Basic ID Segment—The phosphorylation obviously induces the acidic region of dSSRP1 to regulate the DNA binding. However, this region hardly shows any direct interactions with DNA. In fact, the AID proteins (Fig. 1*A*), which mostly consisted of this acidic region, did not interact with 20 bp dsDNA (Fig. 4*A*, *lanes 3* and *4*), whereas the LB-HMG protein (Fig. 1*A*), harboring the basic

phosphoprotein stain kit (Fig. 3*B*), confirming the extremely low level of phosphorylation. These results suggested that the region of amino acids 186–624 of dSSRP1 contains at least ten specific phosphorylation sites, which overall are targeted by CK2.

To investigate whether the phosphorylation within the region of amino acids 186–624 affects the nucleosomal DNA binding activity of dSSRP1, we performed EMSAs using the same mutants of Mid-dSSRP1, as shown in Fig. 3*C*. The 10SA-Mid-dSSRP1 proteins were able to more strongly bind to the 263 bp mononucleosome, in comparison with WT-Mid-dSSRP1 (Fig. 3*C*, *lanes 2* and *3 versus lanes 10* and *11*). The binding abilities of the mutants (2SA, 4SA, 6SA, and 10A-Mid-

segment and its adjoining HMG domain, was able to directly interact with DNA (Fig. 4*A*, *lane 2*). We also found that the basic segment was essential to enhance the affinity for the DNA binding (supplemental Fig. S5). The acidic region and the basic segment are entirely unstructured, as convincingly demonstrated by the high-speed AFM (27) and CD analyses (data not shown). Taken together, it is likely that the acidic ID region makes intramolecular interactions with the HMG domain and the neighboring basic ID segment, thereby conferring inhibitory effects on the DNA binding activity of dSSRP1.

To test this possibility, we analyzed the interaction between the acidic region and the HMG domain within dSSRP1 by EMSAs. The phosphorylated AID protein (Sf9-AID) was obtained by treating Sf9-Mid-dSSRP1 carrying two protease sites with thrombin and factor Xa, as described under "Experimental Procedures." We also confirmed that the Mid-dSSRP1 with two protease sites received almost the same degree of phosphorylation as that of the wild-type protein (data not shown). The Sf9-AID and Eco-AID proteins were able to bind to the LB-HMG protein, and the gel mobilities of these complexes were almost identical to those for the respective AB-HMG proteins (Figs. 1*A* and 4*B*, *lane 2 versus lane 3* (*Eco*); *lane 5 versus lane 6* (*Sf9*)), which are composed of the acidic region, the basic segment and the HMG domain. Chemical cross-linking with EDC was employed to examine the effect of the basic ID segment on the interaction between the HMG domain and the acidic ID region (supplemental Fig. S6). The HMG proteins with the preceding basic ID segment (SB-HMG and LB-HMG; Fig. 1*A*) formed multiple cross-linked complexes with the AID protein, regardless of the phosphorylation (supplemental Fig. S6, *lanes 3–6*), although the HMG protein alone could not (supplemental Fig. S6, *lanes 7* and *8*). Together with the data from the binding analyses, this suggests that the basic ID segment contributes to the intramolecular interaction with the acidic region.

To further investigate the interaction between the acidic region and the HMG domain harboring the basic ID segment, we performed the NMR titration experiment using the AID protein and the ^{15}N-labeled SB-HMG protein, which contains a part of the basic ID segment and the HMG domain (Fig. 5). In the observed chemical shift perturbation profile, significant changes were observed at residues in the basic ID segment upon the binding to the AID protein (Fig. 5*B*, residue numbers from −11 to 0, and Fig. 5*C*, *blue residue numbers*). This finding is consistent with chemical cross-linking experiments described above (supplemental Fig. S6). Amino acids in the HMG domain

also showed clear chemical shift changes by the titration (Fig. 5*B*, residue numbers from 1 to 70). These results suggest that the AID protein interacts with both the basic ID segment and the HMG domain.

Competitive Binding of the DNA Binding Elements between dsDNA and the Acidic ID Region—The above data raise the possibility that both the HMG domain and basic ID segment are involved in competitive binding between the dsDNA and AID protein. To prove this possibility, the complex between the AID and LB-HMG proteins was titrated with up to a 10-fold molar excess of dsDNA (Fig. 6*A*). We observed that the non-phosphorylated Eco-AID protein complexed with the LB-HMG is dissociated upon the addition of an equimolar amount of dsDNA (Fig. 6*A*, *lane 4*, Fig. 6*B*). By contrast, the phosphorylated Sf9-AID protein remained to be associated with the LB-HMG even in the presence of a 10-fold molar excess of dsDNA (Fig. 6*A*, *lane 13*, Fig. 6*B*). These results indicated that the acidic ID region interacts with the basic ID segment or the HMG domain with lower affinity than dsDNA, and hence the addition of dsDNA results in the exclusion of the acidic ID region. However, the phosphorylation intensifies the inhibitory power of the acidic ID region, thereby blocking the interaction between dsDNA and the HMG domain.

The WT and 10SA mutant proteins of Sf9-Mid-dSSRP1 exhibited similar CD spectra (Fig. 7), suggesting that the phosphorylation does not induce any secondary structures in the acidic region. It should be noted that one phosphorylation site adds two negative charges, and thus ten phosphorylation sites increase the negative charges of the acidic ID region by ~1.5-fold. Therefore, it is likely that these phosphate groups strengthen the interactions of the unstructured acidic region with both the HMG domain and the basic ID segment mainly by electrostatic forces.

Maternally Supplied Highly Phosphorylated FACT Is Dephosphorylated during Early Embryogenesis—To confirm the biological significance of the dFACT phosphorylation, we investigated the phosphorylation state of native dSSRP1 in the ovary of the adult female fly and the early stage embryo. The native dSSRP1, extracted from the cytosolic fraction of the ovary with 8 M urea, showed the same gel mobility as that purified from Sf9 cells in native-PAGE (Fig. 8*A*, *lane 2 versus lane 3*). The ovarian dSSRP1 protein after APase treatment exhibited reduced gel mobility as compared with that of the dSSRP1 without the APase treatment (Fig. 2*B*, *lane 2 versus lane 1*), because of the loss of negative charges by the dephosphorylation. These results indicated that the dFACT stored in the ovary is highly

---

FIGURE 5. **NMR titration of SB-HMG with the AID protein.** *A*, residue numbers used in the histograms showing chemical shift differences. The residues in the *gray box* come from the plasmid. The residues in the *blue box* are in the basic segment attached to the HMG domain. The HMG domain contains the residues in the *yellow box*; the positions for three helices identified in the NMR structure (PDB: 1WXL) are shown in *orange* with their helix numbers. *B*, histograms show the chemical shift differences in the SB-HMG induced upon binding with the AID protein. Residue numbers are indicated on the *x* axis. Residue numbers for prolines are indicated with *black circles*. The residues that were not assigned due to signal overlaps or not observed duo to exchange with the solvent at pH 7.5 and at the diluted protein concentration (0.1 mM) are shown with *black squares*. The residues that were not observed in the neutral pH condition even at the higher protein concentration of 1.0 mM are shown with the *black inverted triangles*, although they were assigned in the acidic condition at pH 5.2. The histograms are overlaid with different colors according to the ligand concentrations; the order of the colors for the AID peptide interaction is *black* (0), *red* (0.1), *yellow green* (0.2), *blue* (0.5), *yellow* (1.0), *brown* (1.5), and *violet* (2.0). The *green bars* show the chemical shift differences for the unassigned lysine residues, marked with *N.A. (K)* in *C*. *C*, selected part of SB-HMG spectra during the AID protein titration. The spectra obtained for with 0.0, 1.0, 1.5, and 2.0 equivalents of AID protein are plotted in *black*, *red*, *magenta*, and *green*, respectively. The residue numbers in *blue* are the residues in the basic ID segment. *N.A.* indicates the signal that was not assigned due to the signal overlaps in the ^{13}C dimension in the triple resonance spectra. The three signals marked with *N.A. (K)* were all assigned to the Lys residues between −4 and −7 in the basic segment based on their ^{13}Cα and ^{13}Cβ chemical shift values. The signal from one lysine out of four unassigned Lys residues is not clearly identified in the spectra probably due to the overlap to the other signal.
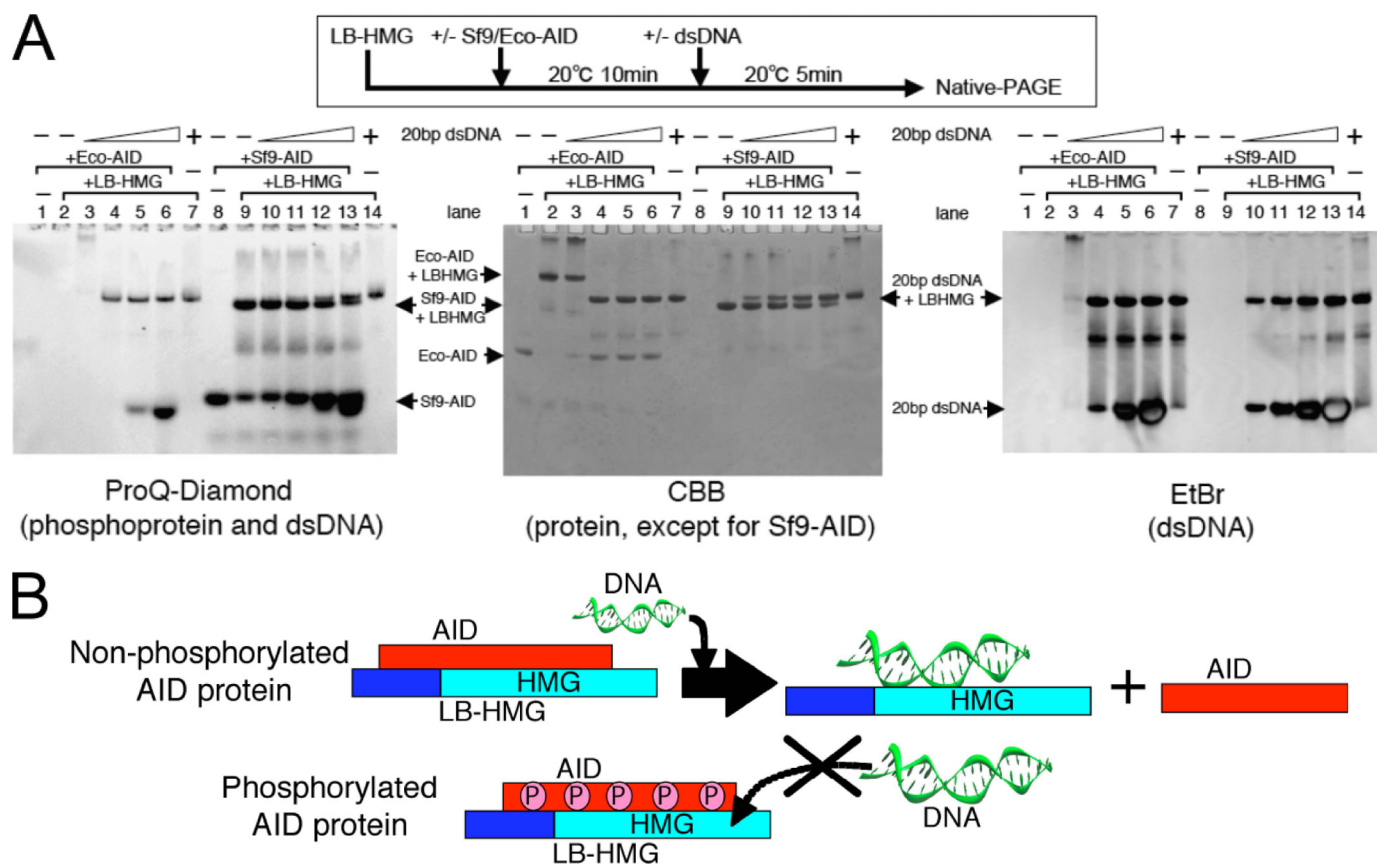
Inhibition by FACT ID Phosphorylation

A

ProQ-Diamond
(phosphoprotein and dsDNA)

CBB
(protein, except for Sf9-AID)

EtBr
(dsDNA)

B

FIGURE 6. **Competitive binding of the HMG domain between dsDNA and the acidic ID region.** *A*, ProQ-Diamond (*left*), CBB (*center*), and EtBr (*right*) staining of the complexes exchanged by dsDNA after 15% native-PAGE. After 0.1 nmol of AID proteins were preincubated with an equimolar amount of LB-HMG for 10 min at 20 °C, the resultant complexes were titrated with 0.3, 1.0, 3.0, and 10.0-fold molar amounts of dsDNA, and then were incubated for 5 min at 20 °C. *B*, diagram shows how the phosphorylated AID protein but not non-phosphorylated protein inhibits DNA binding in *A*.
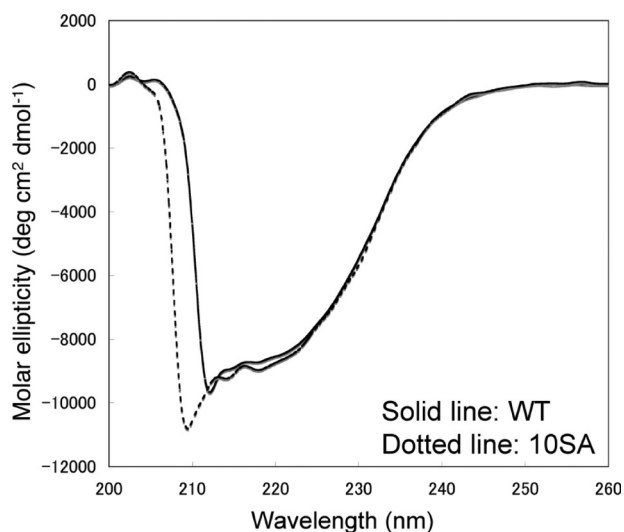

FIGURE 7. **CD analysis of WT and 10SA mutant protein of Sf9-Mid-dSSRP1.** The far-UV CD spectrum (200–260 nm) of the WT protein (*solid line*) is shown in comparison with that of the 10SA mutant protein (*dotted line*). The spectra were measured in buffer A (20 mM Tris-HCl, pH 8.5, 5 mM 2-mercaptoethanol) containing 0.15 M NaCl at 25 °C on a J-725 spectropolarimeter (Japan Spectroscopic Co.). The mean molar ellipticity (deg cm² dmol⁻¹) was calculated by using an average amino acid molecular weight of 110.

FIGURE 8. **Maternally supplied FACT is dephosphorylated at the early embryonic stage.** *A*, analysis for the phosphorylation level of dSSRP1 proteins in the ovary and various stages of the embryo by 5% native-PAGE. The assays were carried out as in Fig. 2*B*, except that dSSRP1 proteins were also extracted from the early stage embryos (0–1, 1–3 h) with 8 M urea. *B*, analysis of the phosphorylation level of dSSRP1 proteins from the cytosolic or nuclear fraction by 5% native-PAGE. The cells were homogenized with the cytosolic extract buffer (50 mM NaCl) and centrifuged, and the supernatant was saved as the cytosolic extract. The nuclear pellet was then treated with the nuclear extract buffer (0.5 M NaCl) to yield the nuclear extract. The assays were identical to those in Fig. 2*B*.

phosphorylated to the same extent as the protein overexpressed in Sf9 cells. On the other hand, the dSSRP1 in the early stage embryos 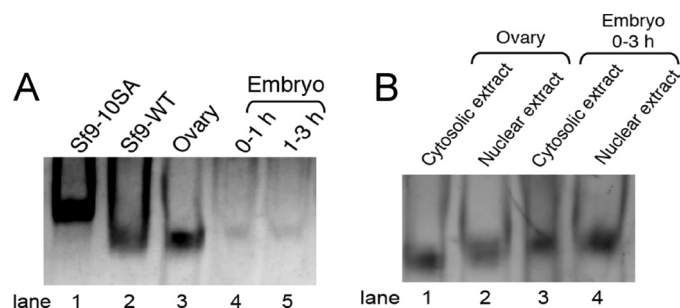(0–1, 1–3 h) showed slightly reduced gel mobility, as compared with the ovarian dSSRP1 (Fig. 8*A*, *lanes 4* and *5 versus lane 3*). Surprisingly, the slight dephosphorylation of dFACT was already completed in the earliest stage 0–1-h embryo (Fig. 8*A*, *lane 4 versus lane 5*). Although the dSSRP1 in the cytosolic extract of the ovary was highly phosphorylated, the nuclear extract showed slight dephosphorylation, presumably reflecting the active dFACT in the nucleus of the ovarian tissue (Fig. 8*B*, *lane 1 versus lane 2*). In the early stage embryo,
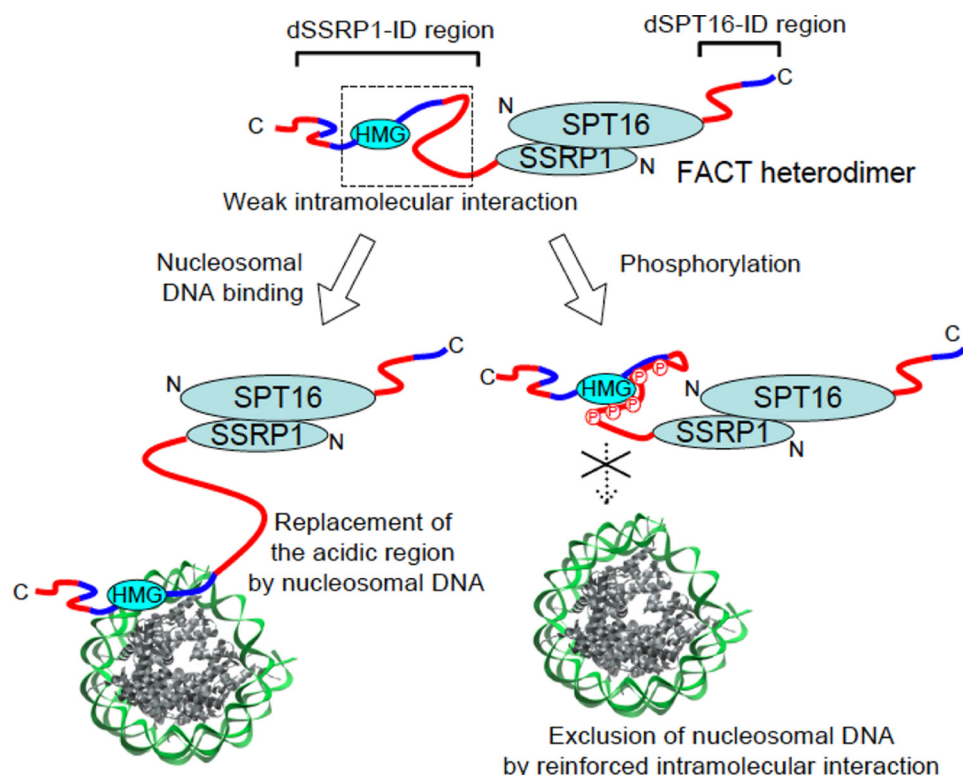
FIGURE 9. **Summary of inhibition mechanism by phosphorylation.** Full-length dFACT contains two tail-like ID regions (*upper*). Within the dSSRP1 ID region, the acidic region forms weak electrostatic interactions with the HMG domain and the basic segment. The nucleosomal DNA binding to both the HMG domain and the basic segment causes exclusion of the acidic region from the complex. Phosphorylation of the acidic region induces stronger intramolecular interactions, thereby blocking DNA binding. The acidic ID region and the following basic ID segment are symbolically represented by the *red* and *blue strings*, respectively. The *P* in *red open circles* indicates the phosphorylation sites. *N* and *C* represent the N and C termini, respectively.

the dSSRP1 from both the cytosolic and nuclear extracts retained almost the same dephosphorylated level (Fig. 8*B*, *lanes 3* and *4*). Collectively, these data suggested that dFACT is stored as the highly phosphorylated inactive form in the oocyte cytoplasm, and is converted into the active form through dephosphorylation immediately after fertilization.

DISCUSSION

The present data provide a mechanistic view of FACT regulation, where the phosphorylation of the ID region prevents the binding between dFACT and the nucleosomal DNA to generate the inactive form for storage (Fig. 9). In the non-phosphorylated state, the acidic ID region forms weak intramolecular interactions with the HMG domain and the neighboring basic ID segment. When the HMG domain and the basic ID segment jointly bind to DNA, the higher affinity for DNA would disrupt the polar interactions of the acidic region with the basic segment. On the other hand, the phosphorylation increases the number of negatively charged groups within the acidic ID region. Presumably, this would result in the reinforcement of the intramolecular interactions, which causes the masking of the DNA binding elements without obvious folding of the ID regions, thereby blocking the DNA binding (Fig. 9). This mechanism relies on the inherent properties of the ID region with the clustered phosphorylation sites, and it should be distinct from the coupled folding that occurs in some proteins upon binding of ID regions.

A similar mechanism could be applied to other proteins, such as HMGB1 and nucleolin. The HMGB1 protein harbors two HMG boxes, A and B, flanked by a basic ID region and a highly acidic C-terminal ID region (37, 38). The acidic region forms intramolecular interactions with the basic region and the HMG domain (39–41). In the maize protein, these interactions were reinforced in response to the phosphorylation of serine residues in the acidic region by CK2, and thus negatively affected the DNA interaction (42). This result is consistent with our mechanism, where the phosphorylated acidic region strongly inhibits the DNA-binding activity. The HMGB1 protein lacking the acidic C terminus repressed the expression of the reporter gene (43). The C-terminal truncation of HMGB1 also inhibited its ability to facilitate the binding of ATP-dependent chromatin remodeling factor to nucleosomal DNA (44). Furthermore, nucleolin, which consists of the N-terminal acidic ID region and the four RNA-binding domains, facilitates transcription through a FACT-like activity (45, 46). A nucleolin mutant, missing the acidic region, exhibited reduced ability to assist nucleosome sliding by SWI/SNF (47). These full-length proteins exhibited lower DNA binding activities than the mutants lacking the acidic regions (43, 44, 47). Together with our present results, these findings imply a common mechanism, where the acidic regions direct the functionally optimal interactions of the adjacent folded domains with DNA.

It has been suggested that protein phosphorylation frequently occurs within ID regions (48, 49). The versatile properties of the ID regions could be easily modified by phosphorylation, and thereby respond to various functional states through intra- and intermolecular recognition. It is intriguing to discuss the functional significance of the phosphorylation in connection with the fly-casting mechanism proposed by Shoemaker *et al.* (50). It appears that the unmodified mode of the dFACT ID region plays a role as the fishing line in the fly-casting mechanism against the nucleosomal DNA, while its phosphorylated form covers the flanking DNA binding elements. The increased capture radius of the unmodified ID region would allow the dFACT protein to search for DNA targets more efficiently. Human CK2 is directly associated with the C-terminal region of hSSRP1 containing the acidic ID region (22). The assembly of the CK2/SSRP1/SPT16 complex and the phosphorylation of SSRP1 are induced in response to UV irradiation (23), and therefore it is likely that the phosphorylation may play some role in modulating the intermolecular interaction between CK2

and hFACT. We anticipate that CK2 may recognize a particular conformation, jointly formed by the HMG domain and the phosphorylated ID region.

Our recent observation by AFM has indicated that the persistent length of the dFACT ID regions is longer than that of random coil protein structures (27). This extended conformation may be more suitable for protein kinases to access target sites. Furthermore, the phosphorylation may expand the ID regions by intensifying their repulsive forces. The ID regions have the propensity to form large interactive surfaces, which allow them to wrap-up or surround their binding partners (51). Consequently, the expanded acidic region could mask both the basic segment and the HMG domain, thus enhancing the inhibitory effect (Fig. 9).

Our study on the phosphorylation states of the native dSSRP1 in the ovary and the early embryo highlighted the physiological importance of this post-translational modification in the FACT protein. UV irradiation reportedly induces hSSRP1 phosphorylation in human cervical carcinoma HeLa cells (8). This FACT phosphorylation may cause global inhibition of transcription or replication by impairing the nucleosomal DNA binding ability of hSSRP. The present study suggested that the cytoplasm of the fly ovary stores dSSRP1 in the highly phosphorylated inactive form. Why does the ovary store the inactive dFACT in the cytoplasm? Within 2 h after fertilization of the oocyte, the early embryo undergoes extremely rapid DNA replication and nuclear division, resulting in a multinucleate cell called a syncytial blastoderm. During the next 2–3 h, the embryo forms a cellular blastoderm, and differentiation is initiated. A large amount of active dFACT is required to support rapid DNA replication and transcription through chromatin remodeling. Therefore, the stored inactive dFACT would be immediately activated by dephosphorylation at the early embryonic stage after fertilization.

Recently, more attention has been focused on the findings that FACT-dependent chromatin remodeling is mechanistically regulated by various post-translational modifications, such as H2B monoubiquitination during transcriptional elongation (7, 52), H2A monoubiquitination in transcription repression (53), and ADP-ribosylation of SPT16 during the DNA repair process (3). The present study illuminates the importance of the phosphorylation states of the dSSRP1 ID region to accommodate the rapid changes in chromatin transactions *in vivo*.

REFERENCES

1. Orphanides, G., Wu, W. H., Lane, W. S., Hampsey, M., and Reinberg, D. (1999) *Nature* **400,** 284–288
2. Reinberg, D., and Sims, R. J., 3rd (2006) *J. Biol. Chem.* **281,** 23297–23301
3. Heo, K., Kim, H., Choi, S. H., Choi, J., Kim, K., Gu, J., Lieber, M. R., Yang, A. S., and An, W. (2008) *Mol. Cell* **30,** 86–97
4. Nakayama, T., Nishioka, K., Dong, Y. X., Shimojima, T., and Hirose, S. (2007) *Genes Dev.* **21,** 552–561
5. Lejeune, E., Bortfeld, M., White, S. A., Pidoux, A. L., Ekwall, K., Allshire, R. C., and Ladurner, A. G. (2007) *Curr. Biol.* **17,** 1219–1224
6. Tan, B. C., Chien, C. T., Hirose, S., and Lee, S. C. (2006) *EMBO J.* **25,** 3975–3985
7. Pavri, R., Zhu, B., Li, G., Trojer, P., Mandal, S., Shilatifard, A., and Reinberg, D. (2006) *Cell* **125,** 703–717
8. Li, Y., Keller, D. M., Scott, J. D., and Lu, H. (2005) *J. Biol. Chem.* **280,** 11869–11875
9. Miles, J., and Formosa, T. (1992) *Proc. Natl. Acad. Sci. U.S.A.* **89,** 1276–1280
10. Formosa, T., Eriksson, P., Wittmeyer, J., Ginn, J., Yu, Y., and Stillman, D. J. (2001) *EMBO J.* **20,** 3506–3517
11. Shimojima, T., Okada, M., Nakayama, T., Ueda, H., Okawa, K., Iwamatsu, A., Handa, H., and Hirose, S. (2003) *Genes Dev.* **17,** 1605–1616
12. Belotserkovskaya, R., Oh, S., Bondarenko, V. A., Orphanides, G., Studitsky, V. M., and Reinberg, D. (2003) *Science* **301,** 1090–1093
13. VanDemark, A. P., Blanksma, M., Ferris, E., Heroux, A., Hill, C. P., and Formosa, T. (2006) *Mol. Cell* **22,** 363–374
14. Stuwe, T., Hothorn, M., Lejeune, E., Rybin, V., Bortfeld, M., Scheffzek, K., and Ladurner, A. G. (2008) *Proc. Natl. Acad. Sci. U.S.A.* **105,** 8884–8889
15. Yarnell, A. T., Oh, S., Reinberg, D., and Lippard, S. J. (2001) *J. Biol. Chem.* **276,** 25736–25741
16. Bruhn, S. L., Pil, P. M., Essigmann, J. M., Housman, D. E., and Lippard, S. J. (1992) *Proc. Natl. Acad. Sci. U.S.A.* **89,** 2307–2311
17. Gariglio, M., Ying, G. G., Hertel, L., Gaboli, M., Clerc, R. G., and Landolfo, S. (1997) *Exp. Cell Res.* **236,** 472–481
18. Schlesinger, M. B., and Formosa, T. (2000) *Genetics* **155,** 1593–1606
19. Cao, S., Bendall, H., Hicks, G. G., Nashabi, A., Sakano, H., Shinkai, Y., Gariglio, M., Oltz, E. M., and Ruley, H. E. (2003) *Mol. Cell. Biol.* **23,** 5301–5307
20. Brewster, N. K., Johnston, G. C., and Singer, R. A. (2001) *Mol. Cell. Biol.* **21,** 3491–3502
21. Krohn, N. M., Stemmer, C., Fojan, P., Grimm, R., and Grasser, K. D. (2003) *J. Biol. Chem.* **278,** 12710–12715
22. Keller, D. M., and Lu, H. (2002) *J. Biol. Chem.* **277,** 50206–50213
23. Keller, D. M., Zeng, X., Wang, Y., Zhang, Q. H., Kapoor, M., Shu, H., Goodman, R., Lozano, G., Zhao, Y., and Lu, H. (2001) *Mol. Cell* **7,** 283–292
24. Dyson, H. J., and Wright, P. E. (2005) *Nat. Rev. Mol. Cell Biol.* **6,** 197–208
25. Dunker, A. K., Lawson, J. D., Brown, C. J., Williams, R. M., Romero, P., Oh, J. S., Oldfield, C. J., Campen, A. M., Ratliff, C. M., Hipps, K. W., Ausio, J., Nissen, M. S., Reeves, R., Kang, C., Kissinger, C. R., Bailey, R. W., Griswold, M. D., Chiu, W., Garner, E. C., and Obradovic, Z. (2001) *J. Mol. Graph Model* **19,** 26–59
26. Liu, J., Perumal, N. B., Oldfield, C. J., Su, E. W., Uversky, V. N., and Dunker, A. K. (2006) *Biochemistry* **45,** 6873–6888
27. Miyagi, A., Tsunaka, Y., Uchihashi, T., Mayanagi, K., Hirose, S., Morikawa, K., and Ando, T. (2008) *Chemphyschem* **9,** 1859–1866
28. Kasai, N., Tsunaka, Y., Ohki, I., Hirose, S., Morikawa, K., and Tate, S. (2005) *J. Biomol. NMR* **32,** 83–88
29. Tsunaka, Y., Kajimura, N., Tate, S., and Morikawa, K. (2005) *Nucleic Acids Res.* **33,** 3424–3434
30. Luger, K., Mäder, A. W., Richmond, R. K., Sargent, D. F., and Richmond, T. J. (1997) *Nature* **389,** 251–260
31. Lowary, P. T., and Widom, J. (1998) *J. Mol. Biol.* **276,** 19–42
32. Dyer, P. N., Edayathumangalam, R. S., White, C. L., Bao, Y., Chakravarthy, S., Muthurajan, U. M., and Luger, K. (2004) *Methods Enzymol.* **375,** 23–44
33. Cavanagh, J., Fairbrother, W. J., Palmer, A. G., III, and Skelton, N. J. (1996) *Protein NMR Spectroscopy*, pp. 411–528, Academic Press, San Diego, CA
34. Delaglio, F., Grzesiek, S., Vuister, G. W., Zhu, G., Pfeifer, J., and Bax, A. (1995) *J. Biomol. NMR* **6,** 277–293
35. Garrett, D. S., Powers, R., Gronenborn, A. M., and Clore, G. M. (1991) *J. Magn. Reson.* **95,** 214–220
36. Ruone, S., Rhoades, A. R., and Formosa, T. (2003) *J. Biol. Chem.* **278,** 45288–45295
37. Grasser, K. D. (2003) *Plant Mol. Biol.* **53,** 281–295
38. Thomas, J. O., and Travers, A. A. (2001) *Trends Biochem. Sci* **26,** 167–174

39. Knapp, S., Müller, S., Digilio, G., Bonaldi, T., Bianchi, M. E., and Musco, G. (2004) *Biochemistry* **43,** 11992–11997

40. Grasser, K. D. (1998) *Trends Plant Sci.* **3,** 260–265

41. Watson, M., Stott, K., and Thomas, J. O. (2007) *J. Mol. Biol.* **374,** 1286–1297

42. Thomsen, M. S., Franssen, L., Launholt, D., Fojan, P., and Grasser, K. D. (2004) *Biochemistry* **43,** 8029–8037

43. Aizawa, S., Nishino, H., Saito, K., Kimura, K., Shirakawa, H., and Yoshida, M. (1994) *Biochemistry* **33,** 14690–14695

44. Bonaldi, T., Längst, G., Strohner, R., Becker, P. B., and Bianchi, M. E. (2002) *EMBO J.* **21,** 6865–6873

45. Mongelard, F., and Bouvet, P. (2007) *Trends Cell Biol.* **17,** 80–86

46. Rickards, B., Flint, S. J., Cole, M. D., and LeRoy, G. (2007) *Mol. Cell. Biol.* **27,** 937–948

47. Angelov, D., Bondarenko, V. A., Almagro, S., Menoni, H., Mongélard, F., Hans, F., Mietton, F., Studitsky, V. M., Hamiche, A., Dimitrov, S., and Bouvet, P. (2006) *EMBO J.* **25,** 1669–1679

48. Collins, M. O., Yu, L., Campuzano, I., Grant, S. G., and Choudhary, J. S. (2008) *Mol. Cell Proteomics* **7,** 1331–1348

49. Iakoucheva, L. M., Radivojac, P., Brown, C. J., O'Connor, T. R., Sikes, J. G., Obradovic, Z., and Dunker, A. K. (2004) *Nucleic Acids Res.* **32,** 1037–1049

50. Shoemaker, B. A., Portman, J. J., and Wolynes, P. G. (2000) *Proc. Natl. Acad. Sci. U.S.A.* **97,** 8868–8873

51. Gunasekaran, K., Tsai, C. J., Kumar, S., Zanuy, D., and Nussinov, R. (2003) *Trends Biochem. Sci.* **28,** 81–85

52. Fleming, A. B., Kao, C. F., Hillyer, C., Pikaart, M., and Osley, M. A. (2008) *Mol. Cell* **31,** 57–66

53. Zhou, W., Zhu, P., Wang, J., Pascual, G., Ohgi, K. A., Lozach, J., Glass, C. K., and Rosenfeld, M. G. (2008) *Mol. Cell* **29,** 69–80

54. Kawabata, T., Fukuchi, S., Homma, K., Ota, M., Araki, J., Ito, T., Ichiyoshi, N., and Nishikawa, K. (2002) *Nucleic Acids Res.* **30,** 294–298